

Ellipsometric studies on mutual diffusion and adhesion development at polymer–polymer interfaces

Satoshi Yukioka*, Kahori Nagato and Takashi Inoue†

Department of Organic and Polymeric Materials, Tokyo Institute of Technology, Ookayama, Meguro-ku, Tokyo 152, Japan

(Received 7 March 1991; accepted 25 March 1991)

Ellipsometry was used to estimate the interface thickness λ between two bulk layers of dissimilar polymers, poly(methyl methacrylate) (PMMA) and poly(styrene-*co*-acrylonitrile) (SAN), as a function of annealing time t above the glass transition temperature T_g . The value of λ was estimated to be around 20 nm at an early stage of annealing and increased with time, e.g. up to 60 nm at 130°C after 12 h for a miscible pair such as PMMA and SAN-25 (AN content = 25 wt%), while it remained constant for an immiscible system such as PMMA/SAN-5, even after long annealing for more than 12 h. For miscible systems, the mutual diffusion coefficient D was obtained from the slope of the λ vs. $t^{1/2}$ plot according to the Brochard theory: $\lambda = 2(Dt)^{1/2}$. The D value was found to be roughly proportional to the thermodynamic driving force $|\chi - \chi_c|$, as has also been predicted by Brochard (χ and χ_c being the Flory interaction parameter at the annealing temperature and at the critical point, respectively). The molecular-weight dependence of D was found to follow the 'slow theory'. Further, to analyse the adhesion development, the results for $\lambda(t)$ were combined with the time variation of adhesive strength $\sigma(t)$ observed by Fowler *et al.* It was found that the late stage could be described well by the reptation theory, $\sigma \propto \lambda^{1/2}$, while the adhesive strength σ of a thin interface at an early stage was much higher than the theoretical value.

(Keywords: diffusion; adhesion; interface; ellipsometry; kinetics; poly(methyl methacrylate); poly(styrene-*co*-acrylonitrile); miscibility)

INTRODUCTION

Study of the interface between dissimilar polymers is an interesting subject, which leads to a better understanding of the adhesion between the two phases and the bulk properties of polymer blends. Various techniques have been developed for investigating the 'thick interface' generated by interdiffusion in miscible polymer–polymer systems^{1–6}. In each case, the interface is set up between two polymer layers and it grows to a layer more than a micrometre thick with annealing at temperatures above the glass transition temperature T_g . The thickness and composition profile of a thick interface have been evaluated by electron microscopy^{1,2}, forward recoil spectroscopy³, Rutherford back-scattering⁴, infrared microdensitometry⁵ and secondary-ion mass spectroscopy⁶. These observations provide information about the late stage of interdiffusion in miscible polymer pairs, resulting in recent discussions on the dynamic aspects of phase dissolution.

In contrast, there have been limited studies on the 'thin interface', of the order of 1–10 nm, which is expected to appear in immiscible polymer pairs and at an early stage in the interdiffusion of miscible pairs. For the thin interface, most of the aforementioned techniques are not adequate because of the low spatial resolution. A

promising approach by ellipsometry has been put forward by Kawaguchi *et al.*⁷. Recently, we revised the experimental procedure to prepare a bilayer specimen for ellipsometry⁸.

In the present paper, we carry out ellipsometric studies on a polymer–polymer interface to discuss the kinetic aspects of interdiffusion and adhesion development.

We employ a poly(methyl methacrylate)/poly(styrene-*co*-acrylonitrile) (PMMA/SAN) system. The combination of PMMA and SAN offers a unique opportunity for experimentation. First, the difference in refractive index between PMMA (1) and SAN (2) is large enough for ellipsometry ($n_2 - n_1 > 0.02$). Secondly, PMMA and SAN have essentially the same glass transition temperature ($T_g \approx 105^\circ\text{C}$), so that there is no serious mismatch in mobility factors. Thirdly, by changing the acrylonitrile (AN) content of SAN, one can select both immiscible and miscible combinations, as demonstrated by the miscibility window in *Figure 1*^{9–12}; SAN is miscible with PMMA when the AN content is in the range of 9.5 to 33 wt%. Further, as indicated by asterisks in the single-phase regime in *Figure 1*, if we prepare a series of SAN specimens with different AN contents and carry out the diffusion experiment at a fixed temperature T , we would be able to observe the effect of the thermodynamic driving force for interdiffusion, i.e. $|T_c - T|$ or $|\chi - \chi_c|$, where T_c is the lower critical solution temperature (LCST) and χ_c is the Flory interaction parameter at T_c .

* On leave from Tosoh Corporation, Yokkaichi, Mie 510, Japan

† To whom correspondence should be addressed

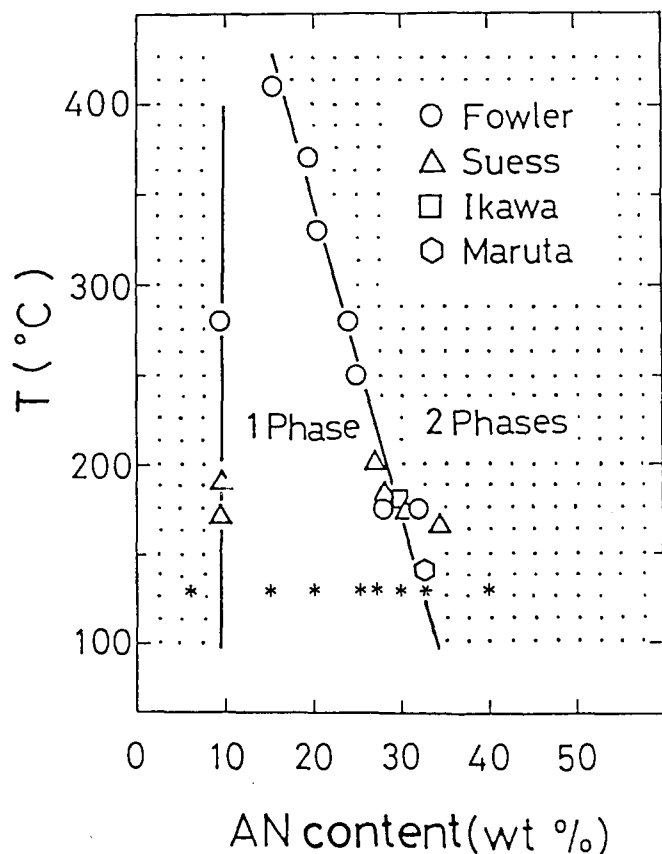


Figure 1 Miscibility window of PMMA/SAN system (from refs. 9-12). Asterisks show the experimental points at 130°C in this study

Table 1 Polymer specimens

Code	AN content (wt%)	$M_w \times 10^{-4}^a$	M_w/M_n^a	n^b
SAN-5	5.7	25.9	2.2	1.583
SAN-15	14.9	14.1	2.6	1.574
SAN-20	19.5	13.0	2.5	1.571
SAN-25	22.3	16.0	2.4	1.571
SAN-27	26.5	10.2	2.9	1.570
SAN-30	30.3	15.5	2.1	1.562
SAN-33	32.3	7.8	2.6	1.560
SAN-40	38.7	7.4	2.2	1.555
PMMA-1	-	1.4	2.1	1.491
PMMA-2	-	2.6	2.0	1.491
PMMA-3	-	7.1	1.8	1.486
PMMA-4	-	15.1	2.1	1.486
PMMA-5	-	39.6	2.7	1.487
PMMA-6	-	82.1	4.0	1.488
PMMA-7	-	7.5	1.9	1.490
PS	-	18.0	2.0	1.590

^aFrom g.p.c.

^bRefractive index by ellipsometry ($\lambda' = 546.1 \text{ nm}$)

EXPERIMENTAL

The polymer specimens used in this study and their characteristics are shown in Table 1. Note that SANs with intermediate AN content (AN = 15-33 wt%) offer miscible combinations with PMMA and SANs with high and low AN contents (SAN-5 and SAN-40) are immiscible with PMMA.

We prepared a bilayer specimen, which consisted of a thin (ca. 600-700 nm) SAN film and a thick (ca. 0.5 mm)

PMMA substrate, by the following procedure⁸. PMMA was melt-pressed between two silicon wafers to form an optically-flat substrate. SAN was dissolved at 6 wt% in chlorobenzene. The solution was filtered through a 0.22 μm Millipore film to remove dust. The filtered solution was spin-coated onto a silicon wafer. The thickness and refractive index of the thin SAN film on the wafer were measured by a stylus method and ellipsometry, respectively. The film edge was scratched with a razor blade and then immersed gently into a water bath. The thin film was floated off onto the water surface as shown in Figure 2a. Then the film was picked up with the PMMA substrate as described in Figure 2b. The bilayer specimen thus prepared was dried under vacuum (10^{-2} Pa) at 60°C for 24 h. We also prepared a bilayer specimen with the opposite configuration, i.e. thin PMMA film on thick SAN substrate.

The bilayer specimen was inserted into a hot chamber kept at 130°C and annealed under a nitrogen atmosphere. Then it was quenched at ambient temperature and served for ellipsometry.

Ellipsometric analysis was carried out by a Shimadzu Ellipsometer, model EP-10, from Shimadzu Manufacturing Co. Ltd. Incident light of 546.1 nm wavelength (λ') was applied to the bilayer specimen at an incident angle of 70° (θ_1). The retardation Δ and the reflection ratio $\tan \psi$ of reflected light were determined from ellipsometric readings.

For data analysis, we used a four-layer model as shown in Figure 3. Since the values of refractive indices n_1 , n_2 and n_4 and thickness d_2 are known, one can estimate n_3

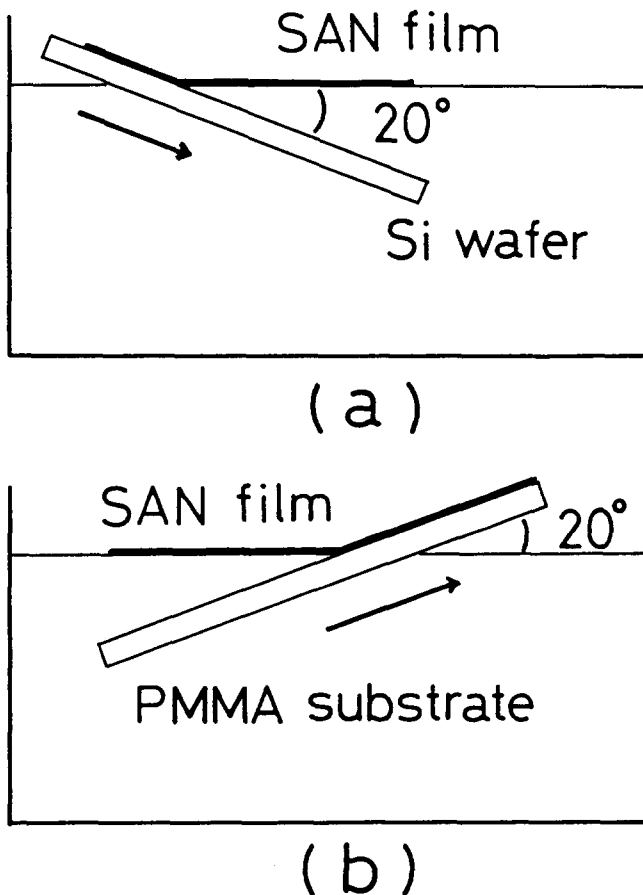


Figure 2 Set-up of bilayer specimen: (a) float off a thin (600-700 nm) SAN film from the silicon wafer onto the water surface and (b) pick up the SAN film with a thick (~0.5 mm) PMMA substrate

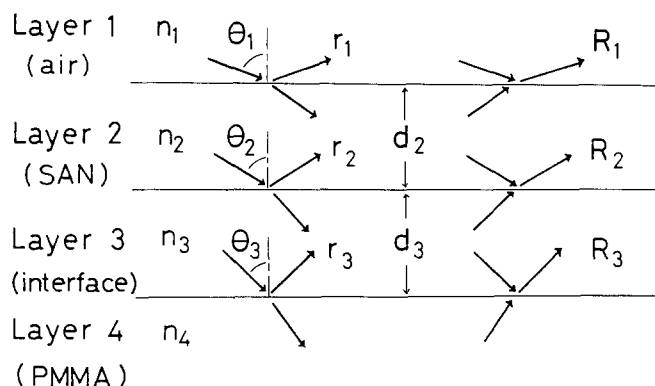


Figure 3 Four-layer model for ellipsometric analysis

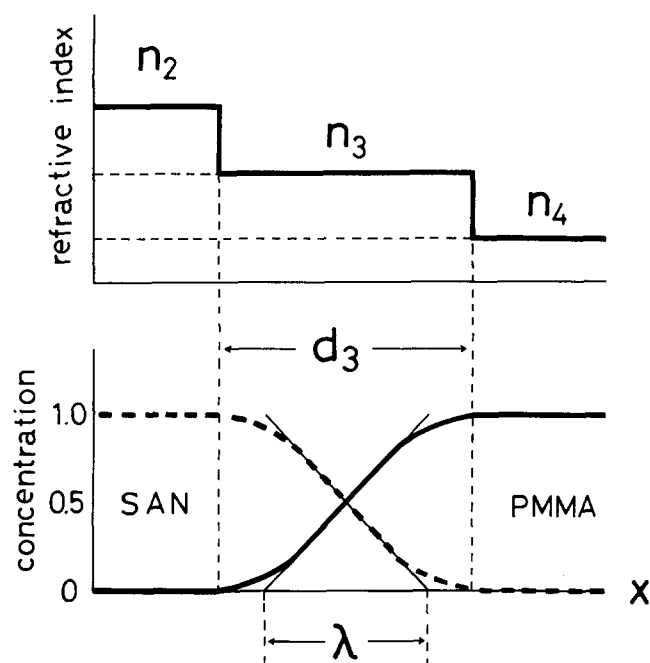


Figure 4 Concentration profile at polymer-polymer interface and a stepwise approximation of refractive index profile for ellipsometry

and d_3 by selecting the best set of these values to fit the observed values of Δ and $\tan \psi$ to the Drude equation¹³ for the four-layer model⁷:

$$\rho = \frac{R_m^p}{R_m^s} = \frac{|R_m^p| \exp(i\Delta_p)}{|R_m^s| \exp(i\Delta_s)} = \frac{|R_m^p|}{|R_m^s|} \exp[i(\Delta_p - \Delta_s)] = \tan \psi \exp(i\Delta) \quad (1)$$

$$R_m^v = \frac{r_m^v + R_{m+1}^v \exp(-iD_{m+1})}{1 + r_m^v R_{m+1}^v \exp(-iD_{m+1})} \quad (v = p, s) \quad (2)$$

$$D_m = 4\pi n_m d_m (\cos \theta_m) / \lambda' \quad (3)$$

where ρ is the relative amplitude of parallel (R_m^p) to perpendicular (R_m^s) reflection coefficients in the incident plane, n_m and d_m represent the refractive index and thickness of the m th layer, respectively, and r_m is the Fresnel reflection coefficient at the boundary between m th and $(m+1)$ th layers:

$$r_m^p = \frac{n_{m+1} \cos \theta_m - n_m \cos \theta_{m+1}}{n_{m+1} \cos \theta_m + n_m \cos \theta_{m+1}} \quad (4a)$$

$$r_m^s = \frac{n_m \cos \theta_m - n_{m+1} \cos \theta_{m+1}}{n_m \cos \theta_m + n_{m+1} \cos \theta_{m+1}} \quad (4b)$$

$$n_1 \sin \theta_1 = n_2 \sin \theta_2 = n_3 \sin \theta_3 = n_4 \sin \theta_4 \quad (5)$$

Numerical calculation for the best fitting was carried out by a Hitachi computer, Hitac M-660K. The four-layer model in Figure 3 implies that the refractive index at the interface is approximated to being uniform and equal to $n_3 = (n_2 + n_4)/2$ (Figure 4). Taking account of the composition profile at the interface layer, the interfacial thickness λ was determined as $\lambda = d_3/1.7$ (Figure 4).

RESULTS AND DISCUSSION

The contiguity of thin film and thick substrate in the bilayer specimen was confirmed by measuring the thickness of the thin film (d_2) by ellipsometry at several positions of the bilayer specimen. That is, the d_2 value was found to be constant everywhere on the thick substrate, and it was exactly equal to that of the thin film on the silicon wafer (measured by stylus method). This implies that the thin film was successfully mounted on and contacted to the substrate without wrinkles and blisters.

Figure 5 shows the typical time variation of interfacial thickness. The results indicated by open circles are for the bilayer specimen composed of thin SAN film and thick PMMA substrate, as illustrated in Figure 5. Full circles in this figure are for the opposite configuration: thin PMMA on thick SAN. The interfacial thickness λ in the immiscible system, SAN-5/PMMA, is around 19 nm. It remains constant even after long annealing for more than 12 h*. A similar result was obtained for

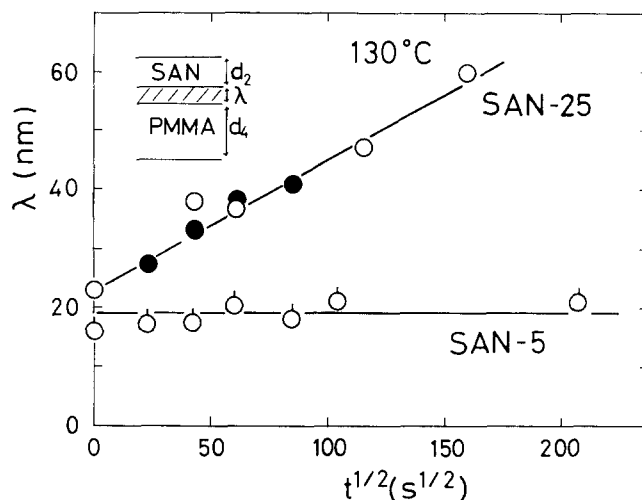


Figure 5 Typical time variations of interfacial thickness in miscible (PMMA/SAN-25) and immiscible (PMMA/SAN-5) systems, for a thick PMMA substrate carrying a thin SAN film. Full circles are for the opposite configuration: PMMA thin film on a thick SAN substrate (see inset to Figure 9)

* The thickness ($\lambda = 19$ nm) in the immiscible system is assumed to be the equilibrium one. However, it is much larger than the theoretical value ($\lambda = 6.4$ nm) according to $\lambda \propto 2b/(6\chi)^{1/2}$, assuming $\chi = 1.05 \times 10^{-2}$ (at room temperature)¹⁴, where b is the Kuhn segment length (≈ 0.8 nm). Taking account of the temperature dependence of χ and hence using smaller χ at the annealing temperature, λ is estimated to be much larger, but is still smaller than the observed value. The reason for this discrepancy is not obvious at present. It should be the subject to discussion after investigating the λ values for various combinations of immiscible polymers

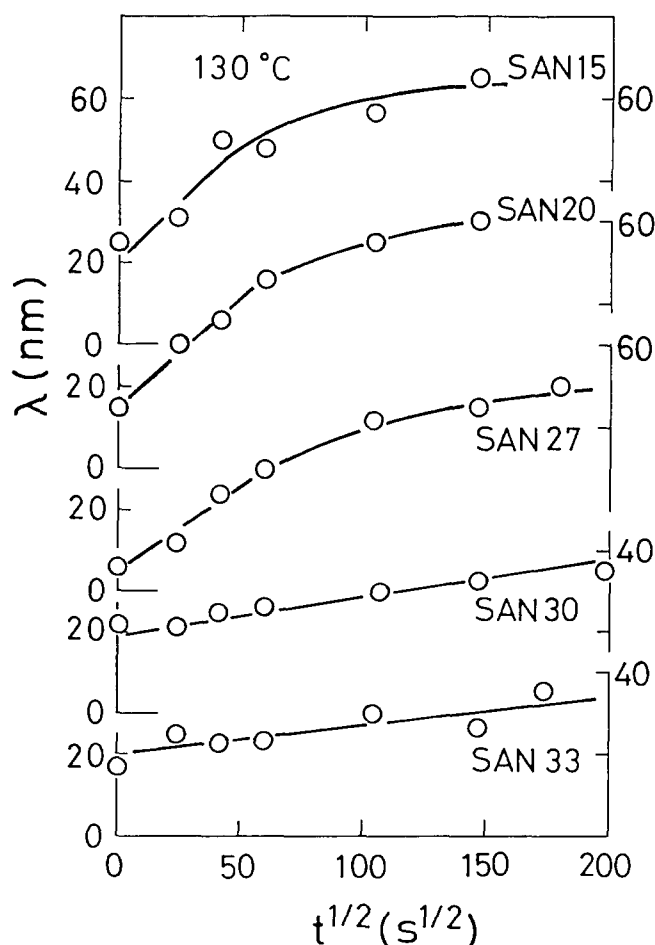


Figure 6 Effect of AN content of SAN on the time variation of interfacial thickness. Molecular weight of PMMA = 7.5×10^4

another immiscible pair, SAN-40/PMMA, in which λ was ca. 30 nm.

In contrast, for the miscible system, SAN-25/PMMA, λ increases with time of annealing up to 60 nm, suggesting the interdiffusion of dissimilar polymers. The same time variation is seen for different configurations (full and open circles). These results may suggest that the interdiffusion process is adequately evaluated by the ellipsometry.

According to the recent theory of polymer-polymer interdiffusion by Brochard *et al.*¹⁵, the time variation of λ is given by:

$$\lambda = 2(Dt)^{1/2} \quad (6)$$

where D is the mutual diffusion coefficient and t is the diffusion time. Then, one can estimate the value of D from the linear plot of λ versus $t^{1/2}$ for the miscible system in Figure 5†.

In Figure 6 are shown the time variation of λ for a series of bilayer specimens composed of thin SAN films and thick PMMA substrate. Here all SANs located in the single-phase region in Figure 1. In all bilayer specimens, λ increases with time of annealing. The larger

† The interface at $t = 0$ has a definite value (λ_0). We have no idea how to interpret it. The origin might be different from the mutual diffusion process above T_g . Then we simply assumed that the linear results in Figure 2 are given as $(\lambda - \lambda_0) \propto t^{1/2}$ and estimated the D value by the slope in Figure 5. When the λ versus $t^{1/2}$ plot deviated from a straight line at late stages (see Figures 6 and 8), we estimated D by the best fitting for $\lambda = 2D^{1/2}(t + t_0)^{1/2}$. The result was almost equal to that from the initial slope of λ versus $t^{1/2}$.

the difference between $LCST$ and annealing temperature ($=130^\circ C$), the faster is the increase in λ . This may suggest that diffusion takes place faster when the thermodynamic driving force for dissolution $|\chi - \chi_c|$ is larger, as predicted by Brochard *et al.*¹⁵:

$$D \propto |\chi - \chi_c| \quad (7)$$

where χ_c is the Flory interaction parameter at $LCST$. The values of D from the slopes in Figure 6 are plotted in Figure 7 as a function of $|\chi - \chi_c|$. Here χ values were estimated by the binary interaction model¹⁶:

$$\chi = BV_r/RT \quad (8a)$$

$$B = B_{13}\phi_1 + B_{23}\phi_2 - B_{12}\phi_1\phi_2 \quad (8b)$$

$$\chi_c = \frac{1}{2}(N_{SAN}^{-1/2} + N_{PMMA}^{-1/2})^2 \quad (8c)$$

where V_r is the molar volume of segment ($=90 \text{ cm}^3 \text{ mol}^{-1}$), B_{ij} is the interaction parameter between components i and j ($1 = \text{styrene}$, $2 = \text{AN}$ and $3 = \text{MMA}$), ϕ_i is the copolymer composition of SAN, and N is the degree of polymerization. Similar plots at $115^\circ C$ are also shown in Figure 7. Data are scattered around the theoretical lines, suggesting that D is roughly proportional to the thermodynamic driving force.

Figure 8 shows the effect of molecular weight on the time variation of λ . Here the bilayer specimens are composed of thin PMMA films, having various molecular weights, and a SAN-25 substrate. The D values from the linear slopes are shown in Figure 9 as a function of the molecular weight of PMMA.

The molecular-weight dependence of D is also predicted

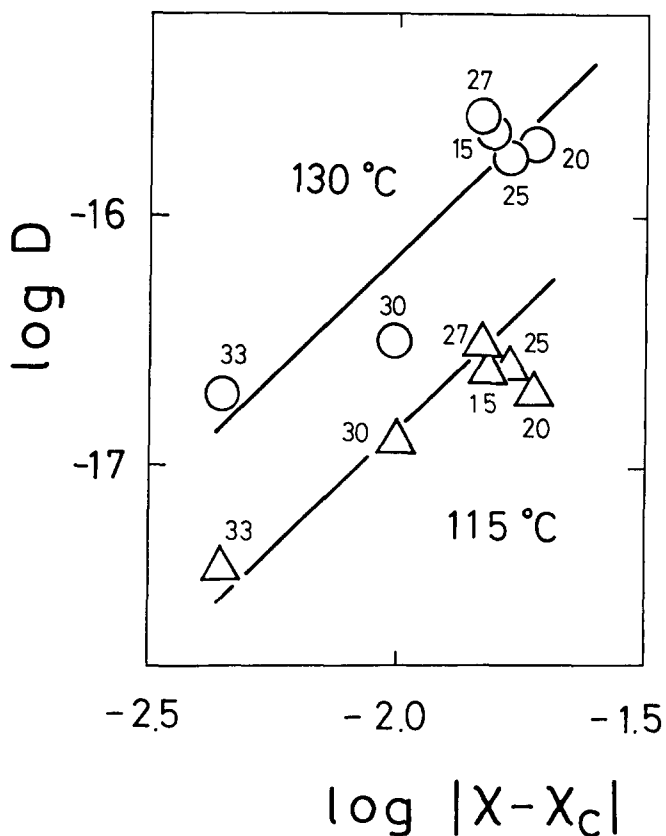


Figure 7 Thermodynamic driving force $|\chi - \chi_c|$ versus mutual diffusion coefficient D . The numbers denote AN content of SAN

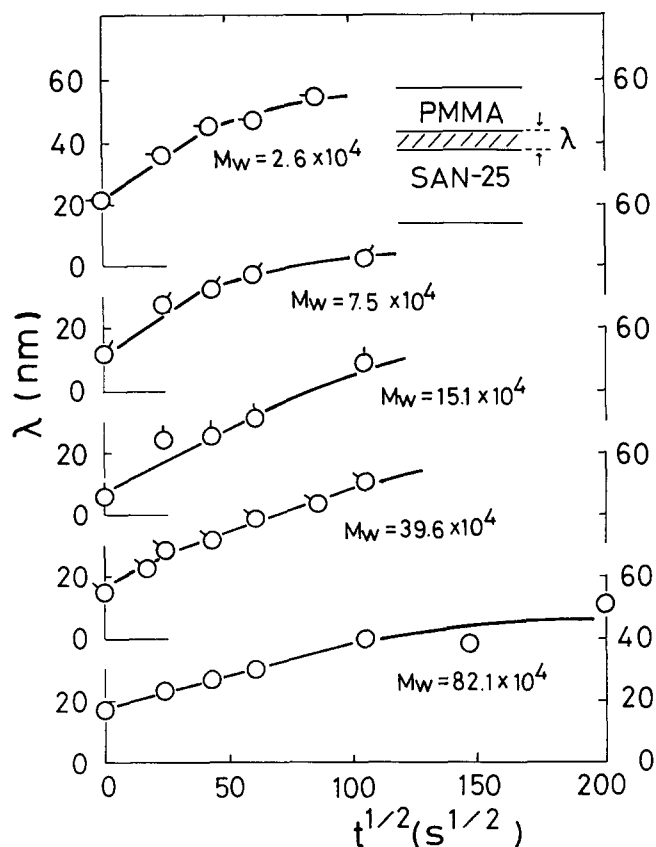


Figure 8 Effect of molecular weight of PMMA on the time variation of interfacial thickness

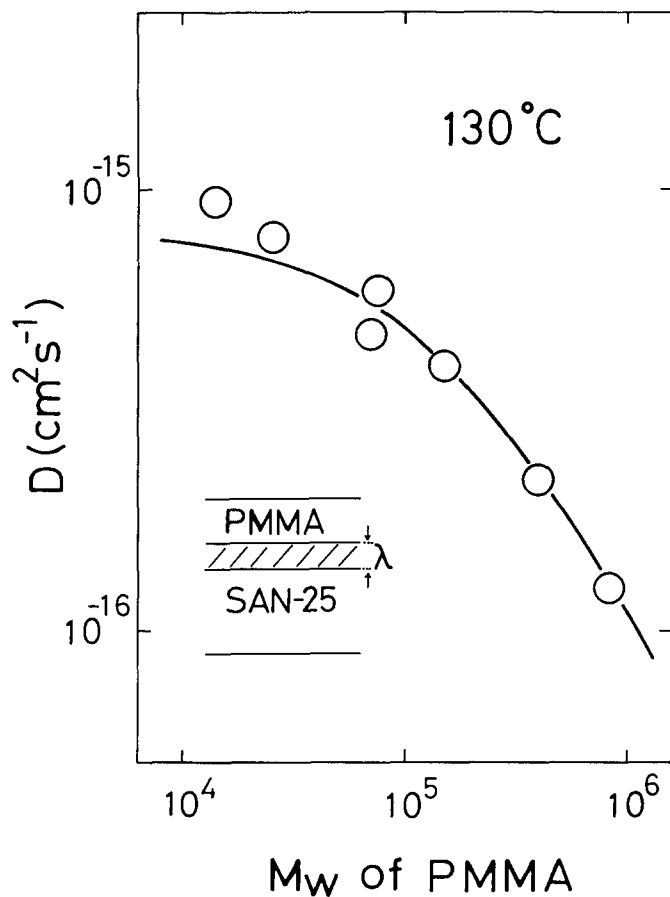


Figure 9 Molecular-weight dependence of the mutual diffusion coefficient

by Brochard *et al.*¹⁵:

$$D \propto (\phi_B M_A + \phi_A M_B)^{-1} \quad (9)$$

where M_i and ϕ_i are the molecular weight and volume fraction of component polymer i , respectively. The full curve in Figure 9 is a plot of equation (9). The molecular-weight dependence of D seems to be well interpreted in the framework of the 'slow theory', which claims that D is mostly governed by the slower moiety.

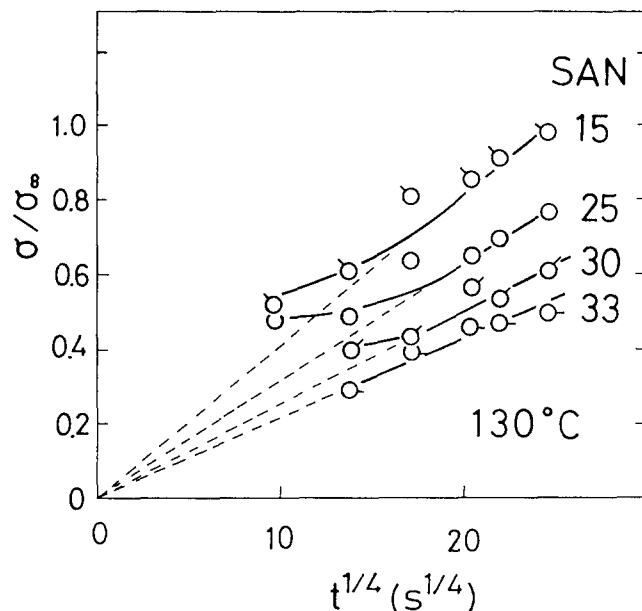


Figure 10 Adhesion development in PMMA and SAN systems, replotted from ref. 17

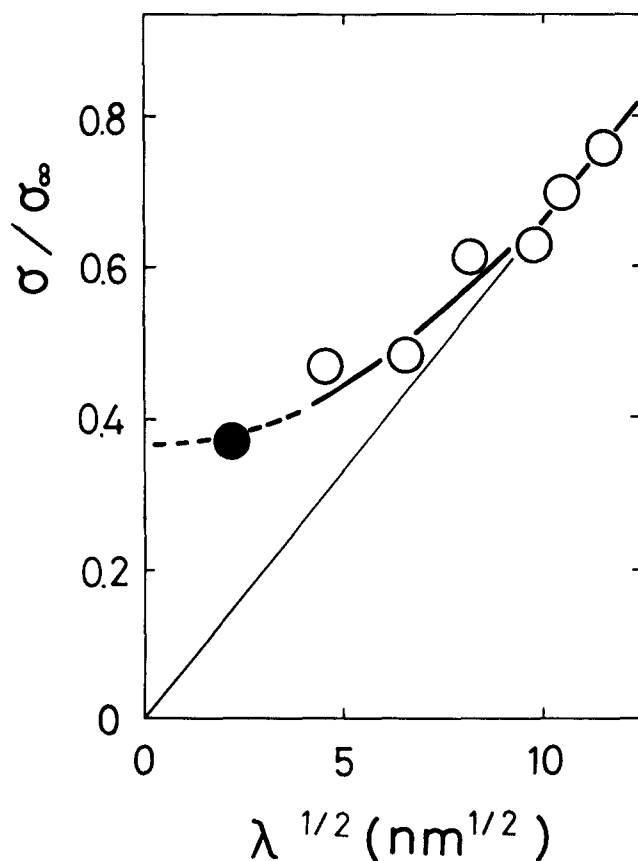


Figure 11 Adhesive strength versus interfacial thickness in PMMA/SAN-25 (○) and PMMA/polystyrene (●)

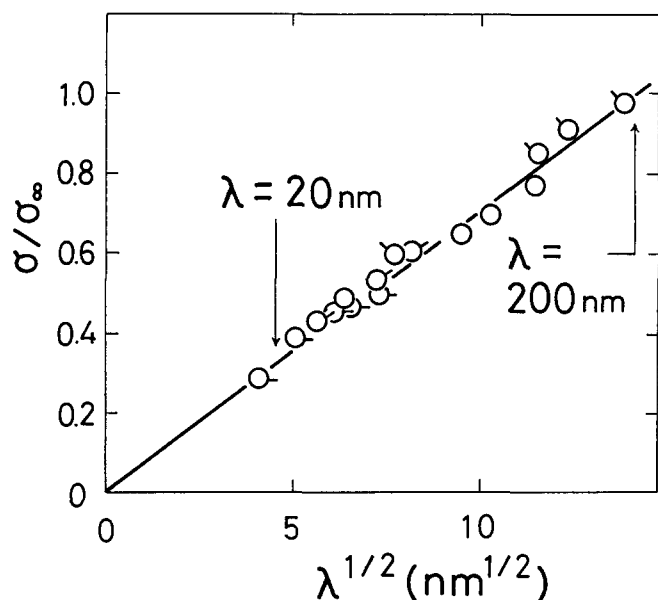


Figure 12 Adhesive strength as a function of interfacial thickness. Symbols are the same as in *Figure 10*

The kinetics of adhesion development at the interface between PMMA and SAN was studied by Fowler *et al.*¹⁷. The results are reproduced in *Figure 10*. Here the adhesive strength σ is normalized by the bulk tensile strength σ_∞ of the weaker material (SAN). Combining the results for $\sigma(t)$ with our results for $\lambda(t)$, one can discuss the adhesion as a function of interfacial thickness. The component polymers in *Figure 10* are slightly different from ours in molecular weight and AN content. However, as has been discussed above, the dependence of D on molecular weight and AN content are given, so that one can analyse the data in *Figure 10* to replot σ as a function of λ . An example is shown in *Figure 11*, assuming $D = 1.29 \times 10^{-16} \text{ cm}^2 \text{ s}^{-1}$ for the PMMA/SAN-25 system. The straight line in *Figure 11* is the result of reptation theory given by Kim and Wool¹⁸:

$$\sigma \propto \lambda^{1/2} \quad (10)$$

As shown in *Figure 11*, the σ of the thick interface seems to be well described by reptation theory, while the thin interface exhibits a much higher σ than the theoretical value. Similar results were obtained for other PMMA/SAN combinations. Omitting the data deviating from the straight lines, the remaining σ values for the thick regime were plotted as a function of $\lambda^{1/2}$. As shown in *Figure 12*, the data points for various PMMA/SAN combinations collapsed onto a straight line. It confirms that the reptation theory is valid for the thick interface ($\lambda > 20 \text{ nm}$) or for the late stage of interdiffusion.

At present, we have no idea how to interpret the deviation from reptation theory for the thin interface, demonstrated typically in *Figure 11*. The van der Waals attraction may contribute significantly to adhesion development. The full circle in *Figure 11* is for an immiscible combination, PMMA/polystyrene, having very thin interface. The point locates just on the extrapolated broken curve, supporting the validity of extrapolation to a thinner interface. It may be an interesting subject in future to accumulate such data and discuss the adhesion at a thin interface.

ACKNOWLEDGEMENTS

We express our appreciation to Professors Akira Takahashi and Masami Kawaguchi, Mie University, for their kind advice on ellipsometry and supplying the computation program. We are also indebted to Dr Yuji Aoki, Mitsubishi Polytech Co., and Mr Masahiko Moritani, Sumitomo Chemical Co., for supplying the SAN and the PMMA specimens, respectively.

REFERENCES

- Gilmore, P. T., Falabella, R. and Laurence, R. L. *Macromolecules* 1980, **13**, 880
- Wu, S., Chuang, H. K. and Han, C. D. *J. Polym. Sci., Polym. Phys. Edn.* 1986, **24**, 143
- Composto, R. J., Kramer, E. J. and White, D. M. *Macromolecules* 1988, **21**, 2580
- Rafailovich, M. H., Sokolov, J., Jones, R. A. L., Krausch, G., Klein, J. and Mills, R. *Europhys. Lett.* 1988, **5**, 657
- Jordan, E. A., Ball, R. C., Donald, A. M., Fetters, L., Jones, R. A. L. and Klein, J. *Macromolecules* 1988, **21**, 235
- Witlow, S. J. and Wool, R. P. *Macromolecules* 1989, **22**, 2648
- Kawaguchi, M., Miyake, E., Kato, T. and Takahashi, A. *Kobunshi Ronbunshu* 1981, **38**, 349
- Yukioka, S. and Inoue, T. *Polym. Commun.* 1991, **32**, 17
- Fowler, M. E., Barlow, J. W. and Paul, D. R. *Polymer* 1987, **28**, 1177
- Suess, M., Kressler, J. and Kammer, H. W. *Polymer* 1987, **28**, 957
- Ikawa, K., Uemura, A., Hosoda, S., Nomura, H., Kojima, T., Chikaishi, K. and Amemiya, Y. *Polym. Prepr. Japan* 1989, **38** (12), 4131
- Maruta, J., Ohnaga, T. and Inoue, T. *Polym. Prepr. Japan* 1989, **38** (10), 3563
- McCrackin, F. L. and Colson, J. P. 'Ellipsometry in the Measurement of Surfaces and Thin Films' (Eds. E. Passaglia, R. P. Stromberg and J. Kurger), NIST Misc. Publ. No. 256, US GPO, Washington, DC, 1964, p. 61
- Helfand, E. and Tagami, Y. *J. Chem. Phys.* 1972, **56**, 3592
- Brochard, F., Jouffroy, J. and Levinson, P. *Macromolecules* 1983, **16**, 1638
- Nishimoto, M., Keskkula, H. and Paul, D. R. *Polymer* 1989, **30**, 1279
- Fowler, M. E., Barlow, J. W. and Paul, D. R. *Polymer* 1987, **28**, 2145
- Kim, Y. H. and Wool, R. P. *Macromolecules* 1983, **16**, 1115